Published in final edited form as:
Biochemistry. 2009 August 4; 48(30): 7169–7178. doi:10.1021/bi900370s.

Roles in Binding and Chemistry for Conserved Active Site Residues in the Class 2 Dihydroorotate Dehydrogenase from *Escherichia coli*

Rebecca L. Fagan[‡] and **Bruce A. Palfey**[*]
Department of Biological Chemistry, University of Michigan Medical School, Ann Arbor, MI 48109-5606

Abstract

Dihydroorotate dehydrogenases (DHODs) catalyze the only redox step in *de novo* pyrimidine biosynthesis, the oxidation of dihydroorotate (DHO) to orotate (OA). During the reaction, the hydrogen at C6 of DHO is transferred to N5 of the isoalloxazine ring of an enzyme-bound FMN prosthetic group as a hydride and an active site base (Ser175 in the Class 2 DHOD from *E. coli*) deprotonates C5 of DHO. Aside from the identity of the active site base, the pyrimidine binding site of all DHODs is nearly identical. Several strictly conserved residues (four asparagines and either a serine or threonine) make extensive hydrogen-bonds to the pyrimidine). The roles these conserved residues play in DHO oxidation is unknown. Site-directed mutagenesis was used to investigate the role of each residue during DHO oxidation. The effects of each mutation on substrate and product binding, as well as the effect on the rate constant of the chemical step were determined. The effects of the mutations ranged from negligible to severe. Some of the residues are very important for chemistry, while others were important for binding. Mutation of residues capable of stabilizing reaction intermediates resulted in large decreases in the rate constant of the chemical step, suggesting these residues are quite important for stabilizing charge build-up in the active site. This finding is consistent with previous results that Class 2 DHODs use a stepwise mechanism for DHO oxidation.

Dihydroorotate dehydrogenases (DHODs[1]) are flavin-containing enzymes that catalyze the fourth step (the only redox step) in the *de novo* synthesis of pyrimidines - the conversion of dihydroorotate (DHO) to orotate (OA) (Scheme 1). DHODs have been categorized into two broad classes based on sequence (1). Several properties of the enzymes segregate nicely into these classes. Class 2 DHODs are membrane-bound enzymes that are oxidized by ubiquinone (2). Class 1 enzymes are cytosolic proteins that have been further divided into two subclasses. Class 1A enzymes are homodimers that are oxidized by fumarate (3). Class 1B enzymes are α_2b_2 heterotetramers that contain a subunit that resembles the Class 1A enzymes and a second subunit that contains FAD and an iron-sulfur cluster, allowing the enzyme to be oxidized by NAD (4). Class 1 DHODs are found mostly in Gram-positive bacteria, although a few microbial eukaryotes also have Class 1A DHODs, while Class 2 enzymes are found in Gram-negative bacteria and almost all eukaryotes.

*To whom correspondence should be addressed at: Department of Biological Chemistry, University of Michigan Medical School, 1150 W. Medical Center Dr., Ann Arbor, MI 48109-5606; Phone: (734) 615-2452; Fax: (734) 764-3509; brupalf@umich.edu.
‡Present Address: Department of Biochemistry, University of Iowa, 51 Newton Rd., Iowa City, IA 52242-1109

SUPPORTING INFORMATION AVAILABLE Reaction traces and concentration dependencies of observed rate constants for the Thr247Ala, Asn177Ala, Asn172Ala\Asn246Ala, Asn111Ala, and Asn11Asp mutant DHODs. This material is available free of charge via the Internet at http://pubs.acs.org.

[1]Abbreviations DHOD, dihydroorotate dehydrogenase DHO, dihydroorotate OA, orotate KIE, kinetic isotope effect k_{red}, reduction rate constant NaP_i, sodium phosphate buffer

The catalytic cycle of DHODs can be studied in two separate half-reactions, allowing the direct observation of the chemistry. The reductive half-reaction involves the oxidation of DHO to OA with the concomitant reduction of the enzyme-bound FMN. The kinetics of the reductive half-reaction has been studied in anaerobic stopped-flow experiments for several Class 2 DHODs (5–7). The spectra of intermediates formed during the reductive half-reaction have been determined (7), allowing a common scheme to be proposed.

Oxidation of DHO breaks two carbon-hydrogen bonds; an active site base deprotonates the C5 *pro-S* hydrogen of DHO (8) and the C6 hydrogen is transferred as a hydride to N5 of the isoalloxazine ring of the flavin. The active site bases differ between classes of DHODs, with Class 1 enzymes using a cysteine and Class 2 enzymes using a serine. The two C-H bonds could break at the same time in a concerted mechanism or sequentially in a stepwise mechanism. If a stepwise mechanism is used, there are two possible intermediates. If deprotonation occurs first, an enolate intermediate will form. However, if hydride transfer occurs first, an iminium intermediate will form.

Using DHO deuterated at the 5-, 6-, or both positions in anaerobic stopped-flow experiments, the Class 2 enzyme from *E. coli* was shown to use a stepwise mechanism for DHO oxidation (5). Interestingly, the Class 1A DHOD from *L. lactis* was shown to use a concerted mechanism (9). Aside from the difference in the active site base, the pyrimidine-binding sites of the two classes are nearly identical (10–13). Even though the main structural difference between the enzymes is the base, the identity of the active base is not responsible for the determining the mechanism of DHO oxidation; the *L. lactis* Cys130Ser mutant enzyme was shown to use a concerted mechanism for DHO oxidation (9).

All DHODs contains a ring of strictly conserved asparagine residues that make extensive interactions with OA in the product complex (Figure 1). Also hydrogen-bonding to OA is either a threonine (in Class 2 and 1B enzymes) or a serine (in Class 1A enzymes). In this work, the roles of these highly conserved residues in the Class 2 enzyme from *E. coli* were investigated by site-directed mutagenesis. Most mutations had little effect on the reduction potential of the enzymes, while effects on the kinetics of the reductive half-reaction varied from mild to severe. Our results help define the roles of the conserved active site residues and indicate important differences to the Class 1A enzymes whose structures are very similar.

Experimental Procedures

Site-Directed Mutagenesis

Site-directed mutants were made from the previously created pAG-1 expression vector (14) using Stratagene QuikChange II XL mutagenesis kit. Insertion of the correct mutation was checked by sequencing the entire pyrD gene.

Overexpression and Purification of DHODs

Wild-type *E. coli* DHOD and all mutant enzymes were overexpressed in *E. coli* strain SØ6645 (a DHOD deletion strain) as previously described (14). All proteins were purified using previously published procedures (14). All purified enzymes were diluted to 50% (v/v) glycerol and stored at −80 °C. Enzymes were exchanged into the correct buffer for experiments using Econo-Pac 10DG disposable desalting columns (Bio-Rad).

Instrumentation

Absorbance spectra were obtained using a Shimadzu UV-2501PC scanning spectrophotometer. Stopped-flow experiments were performed at 4 °C using a Hi-Tech Scientific KinetAsyst SF-61 DX2 stopped-flow spectrophotometer.

Preparation of Anaerobic Solutions

Enzyme solutions for rapid-reaction studies were made anaerobic in glass tonometers by repeated cycles of evacuation and equilibration under an atmosphere of purified argon as previously described (15). Substrate solutions were made anaerobic within the syringes that were to be loaded onto the stopped-flow instrument by bubbling solutions with purified argon. Slow reactions were performed in anaerobic cuvettes (16) and monitored in a standard scanning spectrophotometer. These reaction mixtures were also made anaerobic by repeated evacuation and equilibration with purified argon.

Reduction Potentials

Reduction potentials were determined by the xanthine/xanthine oxidase method of Massey (17). Experiments were preformed in anaerobic cuvettes (16) and monitored in a standard scanning spectrophotometer. 1-Anthraquinone sulfonate (E_m = −225 mV), phenosafranin (E_m = −252 mV), and benzyl viologen (E_m = −350 mV) were used as indicator dyes.

OA Binding to Oxidized DHODs

To increase the solubility of OA, the Tris salt was prepared. The sodium salt of OA from Sigma-Aldrich (31.2 g; 175 mmol) in 500 mL isopropanol was brought to a boil. 24.6 g (203 mmol) of Tris base in 80 mL H_2O was slowly dripped into the solution and the reaction was refluxed overnight. The mixture was then filtered and the solid was dried. The remaining white precipitate was the OA-Tris salt and was soluble in water to at least 400 mM.

The affinity of the oxidized enzymes for OA was determined in aerobic titrations in a standard scanning spectrophotometer at 25 °C. The enzyme equilibrated in 0.1 M Tris-HCl, pH 8.5 was titrated with OA in the same buffer. The differences in flavin absorbance caused by binding of OA were plotted against OA concentration, and the data were fit to a hyperbola in Kaleidagraph (Synergy, Inc.) to determine the K_d. When ligand binding was tight, data were fit to Equation 1, where E_0 is the total enzyme concentration and L_0 is the total added ligand concentration.

$$\Delta A=\Delta A_{\max}\left[\frac{E_0+L_0+K_d-\sqrt{(E_0+L_0+K_d)^2-4E_0L_0}}{2}\right] \quad \text{(Eq. 1)}$$

Reductive Half-Reactions of Mutant DHODs

The reductive half-reaction of all mutant DHODs except Asn172Ala/Asn246Ala were investigated in anaerobic stopped-flow experiments. The experiments were conducted at 4 °C to facilitate comparison with wild-type. Anaerobic enzyme equilibrated in 0.1 M Tris-HCl, pH 8.5 was mixed with anaerobic DHO in the same buffer (ranging from 40 μM to 300 mM after mixing, depending on the particular mutant enzyme). Even at the highest DHO concentrations, the pH of the final mixtures was shown to be within ~0.1 pH units of pH 8.5. Flavin spectral changes were routinely followed at 450 nm, 475 nm, and 550 nm. For the Asn246Ala mutant enzyme, the reaction was also followed at 510 nm. Reaction traces were fit to sums of either two or three exponentials with Program A (R. Chang, C.-J. Chiu, J. Dinverno, and D. P. Ballou, University of Michigan) depending on the number of phases observed. In all cases the observed rate constant of the phase representing flavin reduction varied hyperbolically with DHO concentration. The reduction rate constant (k_{red}, the limiting value of the observed rate constant at an infinite DHO concentration) and the apparent $K_{d,DHO}$ (the half-saturating concentration) were determined by fitting k_{obs} versus DHO concentration to a hyperbola in Kaleidagraph (Synergy, Inc.).

The reductive half-reaction of the Asn172Ala/Asn246Ala double mutant enzyme was extremely slow. The reaction of this enzyme with DHO was therefore studied using a standard scanning spectrophotometer. Enzyme equilibrated in 0.3 M Tris-HCl, pH 8.5 was mixed with varying concentrations of DHO (40 – 200 mM) in an anaerobic cuvette at either 4 °C or 25 °C and spectra were taken at intervals until the flavin was fully reduced. Reaction traces at 453 nm (the maximum flavin absorbance) were extracted and fit to a single exponential.

Kinetic Isotope Effects on Flavin Reduction

Kinetic isotope effects (KIEs) on flavin reduction were determined using 5,5,6-$^2H_3$ DHO. Deuterated DHO was synthesized according to published procedures (8). Deuterium content was determined using proton NMR spectroscopy. The synthesized substrate was found to be >95 % isotopically pure.

Isotope effects on some enzymes (wild-type, Asn177Ala, and Thr247Ala) were determined in stopped-flow experiments. Anaerobic enzyme equilibrated in 0.1 M Tris-HCl, pH 8.5 was mixed with anaerobic unlabeled or labeled DHO in the same buffer. Reaction traces were collected at 475 nm. The slow reactions of other mutant enzymes were studied in anaerobic cuvette experiments in the same buffer by taking spectra at intervals in a standard scanning spectrophotometer at 4 °C. Flavin absorbance changes at ~450 nm were extracted to give reaction traces. Reaction traces for all enzymes were fit to sums of exponentials using Kaleidagraph (Synergy, Inc.). For wild-type and the Asn177Ala mutant enzymes, saturating 5,5,6-$^2H_3$ DHO was practical, and the reduction rate constant (k_{red}) was determined as described above. For the enzymes where saturation was not practical, DHO concentrations below K_d were used, so the observed rate constants report on k_{red}/K_d. KIEs were calculated by dividing the k_{red} or k_{red}/K_d values obtained with protio-DHO by those determined with 5,5,6-$^2H_3$ DHO.

Results

The side-chains of five strictly conserved residues form hydrogen bonds to pyrimidine ligands in Class 2 DHODs. Each of these residues could have different roles in the binding of DHO and in stabilizing the charged intermediate (enolate or iminium) suggested by deuterium isotope effects (5). These residues – four asparagines and a threonine – were each singly mutated to alanine. The threonine was also mutated to serine because that is the homologous residue in Class 1A DHODs. Additionally, a double-mutant (Asn172Ala/Asn246Ala) was constructed with the goal of determining whether the hydrogen bonds from the two residues to the potential enolate intermediate were synergistic. The effects of the mutations on the thermodynamic properties and reductive half-reaction were determined in detail.

Reduction Potentials

The reduction potential of wild-type and mutant DHODs was determined using the xanthine/xanthine oxidase method of Massey (17). The Class 2 DHOD from *E. coli* was previously reported to have a reduction potential of −310 mV (7) using the Massey method. The reduction potential was determined again using two different indicator dyes, phenosafranin (E_m = −252 mV) and 1-anthraquinone sulfonate (E_m = −225 mV) (Figure 2). In both cases, the reduction potential was found to be ~ −229 mV (Table 1). This value is much higher than the previously reported reduction potential and is near the potential reported for the Class 1A DHOD from *L. lactis* (18). To resolve this contradiction, an anaerobic reaction containing 15 μM NADH, ~0.1 μM Class 1B DHOD, 0.5 μM DHO, and 15.5 μM wild type *E. coli* DHOD in 0.1 M NaP_i, pH 7.0 at 25 °C was observed spectroscopically. The Class 1B enzyme shuttled reducing equivalents from NADH to the *E. coli* enzyme via the catalytic amount of the DHO/OA couple. After 10 minutes, the NADH was fully oxidized and the *E. coli* DHOD was completely reduced.

This result is incompatible with a potential of −310 mV for the *E. coli* enzyme since the potential of the NAD/NADH couple is −320 mV. Therefore, we conclude that the reduction potential of the *E. coli* enzyme is −229 mV.

The reduction potential of most active site mutant enzymes was determined by the xanthine/xanthine oxidase method using either phenosafranin, 1-anthraquinone sulfonate, or both as the indicator dye. Most of the mutations had little effect on the potentials (Table 1). However, the reduction potentials of the Asn177Ala and the Asn172Ala mutant DHODs were ~25 mV lower than that of wild-type. A major change in reduction potential was observed in the Asn111Asp mutant enzyme. To obtain the potential of this enzyme, benzyl viologen (E_m = −350 mV) was used as the indicator dye. This enzyme has a potential of −340 mV, over 100 mV lower than the value determined for wild-type.

OA Binding to Oxidized Enzymes

The UV-visible absorbance spectrum of each oxidized enzyme studied was nearly identical to that of wild-type. The Asn111Asp mutant enzyme, where a negative charge was introduced to the active site, exhibited a minor 1 nm red-shift in the visible maximum flavin absorbance when compared to wild-type. The maximum flavin absorbance of the Asn172Ala/Asn246Ala mutant enzyme was at 453 nm, blue-shifted 3 nm compared to wild-type.

A large red-shift is observed upon OA binding to oxidized Class 1A and Class 2 DHODs (14,18–21). The maximum flavin peak in the *E. coli* DHOD shifts from 456 nm to 475 nm. This spectral change can be used to track OA binding in titration experiments, allowing the determination of OA binding affinity (Figure 3). The dissociation constant of OA for the Class 2 DHOD from *E. coli* was previously reported to be 5 μM at pH 8, 25 °C (14). All the K_d measurements in this work were done at pH 8.5, 25 °C; therefore, the dissociation constant of wild-type *E. coli* DHOD for OA was determined under these conditions and was found to be 3.4 ± 0.8 μM, very similar to the value determined at pH 8.

The effects on OA binding observed in the mutant enzymes varied widely. The conservative mutation, Thr247Ser, had little effect on OA binding (Table 2; Figure 3). When each of the active site residues that hydrogen-bond to OA in the oxidized enzyme-OA structure were mutated to alanine, the largest effects were observed at Asn172 (65-fold weakening) and Asn246 (150-fold weakening), the two residues that interact with the C4 carbonyl of OA. All the alanine single-mutant enzymes exhibited the signature red-shift associated with OA binding.

When both residues that hydrogen-bond to the C4 carbonyl were mutated to alanine (Asn172Ala/Asn246Ala double mutant), the observed K_d sky-rocketed to ~50 mM. The flavin peak did not shift to 475 nm upon OA binding as seen in wild-type and the alanine single-mutant enzymes. Instead a very slight red-shift from 456 nm to 458 nm was observed. No red-shift in the maximum flavin absorbance was observed when the Asn111Asp mutant enzyme was titrated with OA. Due to the limited solubility of OA, the enzyme could only be titrated up to ~75 mM OA. At the highest concentration of OA, the flavin peak exhibited a slight red-shift. However, saturation of OA could not be reached and a K_d >> 75 mM is therefore estimated.

Reductive Half-Reaction of Mutant DHODs

The catalytic cycle of DHODs can be broken down into half-reactions, allowing the individual reactions to be studied in more detail. By studying the reductive half-reaction in the absence of an oxidizing substrate, the oxidation of DHO to OA and concomitant reduction of the enzyme-bound flavin can be observed directly, allowing the determination of the rate constant

of the chemical step. The reductive half-reaction of the Class 2 DHOD from *E. coli* has been previously studied (5,7). Here, we investigated the reductive half-reaction of various active site mutant enzymes in anaerobic stopped-flow experiments to better understand the role each residue plays in catalysis.

All the mutant enzymes studied, except Asn246Ala which will be discussed later, fit the same reaction scheme (Scheme 2) previously proposed for the reductive half-reaction of the wild-type enzyme (7). DHO binding was very rapid and occurred in the dead time of the stopped-flow instrument, causing the flavin absorbance maximum of the free enzyme (~456 nm) to shift to the red in most of the mutant enzymes. In the wild-type enzyme, the flavin peak shifts from 456 nm to 475 nm (5,7). In the mutant enzymes, the maximum depended on the particular mutation, with the flavin peak shifting to anywhere between 466 nm and 475 nm. Only the most extreme mutations – the Asn172Ala/Asn246Ala double-mutant enzyme in which three hydrogen bonds to DHO were removed and the Asn111Asp mutant enzyme in which negative charge was added to the active site – did not exhibit a spectral shift upon DHO binding. Similar red-shifts in the flavin absorbance have been observed for DHO binding in Class 1A and other Class 2 DHODs (5,9).

The reaction traces for each mutant enzyme were fit to sums of exponentials. In all cases, a phase consisting of a large decrease in flavin absorbance at 450 nm and/or 475 nm represented flavin reduction. The observed rate constant of this phase varied hyperbolically with DHO concentration allowing the determination of the reduction rate constant (k_{red}) by extrapolating to saturating DHO, and the K_d of DHO, the half-saturating concentration. A wide range of effects on chemistry was observed (Table 3). On one extreme, the conservative mutation, Thr247Ser barely altered the kinetics from those of the wild-type enzyme (Figure 4). In contrast, flavin reduction in the Asn172Ala mutant enzyme was much slower, with a k_{red} of $0.00437 \pm 0.00002\ s^{-1}$, ~10000-fold slower than the wild-type enzyme (Figure 5). The Asn172Ala/Asn246Ala double-mutant enzyme, which was constructed with the hope of detecting possible synergistic effects of two potentially anion-stabilizing residues, was the slowest mutant enzyme examined. The binding of DHO was so weak, and its reaction was so slow, stopped-flow experiments were not practical. Instead, it was examined at 25° in a standard scanning spectrophotometer.

When flavin reduction occurred quickly (faster than $5\ s^{-1}$), the reduced-enzyme•OA complex could accumulate enough to be observed at 550 nm due to charge-transfer absorbance from the electron-poor product OA stacking against the electron-rich reduced flavin. This charge-transfer absorbance is observed in wild-type enzyme (5,7). As the flavin is reduced, absorbance at 550 nm increases as the reduced enzyme•OA complex forms and then decreases as the product is released. Charge-transfer absorbance was only observed during the reductive half-reaction of the Thr247Ser (Figure 4) and Thr247Ala mutant enzymes. In the other mutant enzymes, flavin reduction was considerably slower and the reduced enzyme•OA complex never accumulated, presumably because the rate constant for flavin reduction was much lower than that of product release. The observed rate constants corresponding to charge-transfer disappearance (product release) in the mutant enzymes where it could be observed decreased with increasing DHO concentration. This concentration dependence is also observed in the wild-type enzyme (7) and indicates a unimolecular step (OA release) preceding a bimolecular step (DHO binding to the reduced enzyme); at high DHO concentrations, the release of OA determines the rate of charge-transfer loss. The rate constant obtained at saturating DHO concentrations for the Thr247Ser mutant enzyme was $\sim 0.4\ s^{-1}$ (Figure 4). The final dead-end reduced-enzyme•DHO complex is not physiologically relevant; it occurs because the large amount of unreacted DHO competes with the small amount of product for the reduced enzyme.

Occasionally, a small phase was observed representing less than 10% of the total absorbance decrease of oxidized flavin. The observed rate constant for this phase was independent of DHO concentration. A similar phase is observed in the reductive half-reaction of wild-type (7). It is unclear what this phase represents. This phase could represent the slow reduction of a small amount of damaged enzyme or the reduction of a small amount of contaminating free flavin. The former idea was supported by experiments with the Thr247Ala mutant enzyme; the difference between the spectra recorded before and after this slow phase clearly indicated the reduction of a red-shifted flavin, which would only be possible with ligand-bound enzyme. Whatever is responsible for this slow phase, the rate constant was always at least an order of magnitude smaller than flavin reduction and product release.

The data obtained with the Asn246Ala mutant enzyme did not fit the same scheme as the other mutant enzymes. When the Asn246Ala mutant enzyme was mixed anaerobically with low mM concentrations of DHO, no red-shift was observed in the maximum flavin absorbance. However, when very high concentrations of DHO were used (40 – 200 mM DHO after mixing), a small red-shift was observed. The reaction traces consisted of three phases at high DHO concentrations. The first observed phase was a mixing artifact caused by the large viscosity difference between the enzyme solution and the extremely high concentrations of substrate being used; it ended after 5 ms (Figure 6B). The second phase was seen as a small decrease in absorbance at 450 nm (Figure 6A and 6B) and a small increase in absorbance at 510 nm. This phase represented the spectral shift associated with substrate binding; the maximum change in absorbance observed when DHO or OA binds to oxidized DHODs typically occurs at ~510 nm. In all other DHODs studied, DHO binding is extremely fast and this spectral shift is complete in the dead-time of the stopped-flow instrument. The final phase of the Asn246Ala reductive half-reaction consisted of a large decrease in absorbance at 450 nm and was assigned to flavin reduction (Figure 6A and 6B).

The reaction traces were fit to the sum of three exponentials. The observed rate constant of the first phase – the mixing artifact - is meaningless, but was fit to ensure proper fitting of the other phases in the traces. The observed rate constant of the second phase, which accompanies the spectral shift caused by DHO binding, was scattered about 10 s^{-1} (Figure 6C). If this phase simply represented DHO binding to the oxidized enzyme, the dependence on DHO concentration would be linear. Therefore, a more complex scheme is needed. Oxidized enzyme existing in equilibrium between two states – a form that can bind DHO and a form that cannot – could explain this observation if a large proportion of the starting enzyme is in the form incapable of binding DHO (Scheme 3). Simulations of the reductive half-reaction using this mechanism result in traces very similar to what was observed experimentally. A similar mechanism has been invoked in the reductive half-reaction of α-glycerol phosphate oxidase (22). The observed rate constant of the final phase, representing flavin reduction, varied hyperbolically with DHO concentration giving a k_{red} of 0.081 ± 0.002 s^{-1} and a half-saturating value of 47 ± 3 mM (Figure 6D). If the mechanism described above is correct, then the apparent $K_{d,DHO}$ would be affected by the equilibrium constant of the conformational change, making the actual $K_{d,DHO}$ lower than the observed half-saturating concentration (Equation 2):

$$K_{d,app} = (1+1/K_{iso})\, K_{d,DHO} \quad \text{(Eq. 2a)}$$

$$K_{iso} = [DHOD_{ox}]^{*} / [DHOD_{ox}] \quad \text{(Eq. 2b)}$$

Kinetic Isotope Effects

The large effects observed on k_{red} for many of the mutant enzymes conceivably could be caused by a rate-determining conformational change. Therefore, KIEs were used to determine whether a non-chemical step was masking the actual rate constant of flavin reduction. KIEs were determined either by measuring k_{red} (by saturating with labeled and unlabeled DHO) or at concentrations below K_d, by measuring k_{red}/K_d. To maximize sensitivity, 5,5,6-$^2H_3$ DHO was used as the labeled substrate. Fast reactions were preformed in anaerobic stopped-flow experiments at 4 °C.[2] Slow reactions were performed in anaerobic cuvettes on a standard scanning spectrophotometer at 4 °C. In all enzymes examined, substantial KIEs were observed: wild type, $^Dk_{red} = 5.3 \pm 0.3$; Thr247Ala, $^D(k_{red}/K_d) = 6.3 \pm 0.4$; Asn177Ala, $^Dk_{red} = 5.9 \pm 0.2$; Asn246Ala, $^D(k_{red}/K_d) = 6.3 \pm 0.4$; Asn111Ala, $^D(k_{red}/K_d) = 5.9 \pm 0.3$; Asn111Asp, $^D(k_{red}/K_d) = 5.3 \pm 0.2$. The substantial isotope effects show that chemistry is determining the rate of reduction in all these enzymes.

Discussion

DHODs catalyze the conversion of DHO to OA with the concomitant reduction of the enzyme-bound FMN prosthetic group. The pyrimidine-binding pockets of Class 1 and Class 2 DHODs are very similar. Several conserved residues that hydrogen bond to the pyrimidine substrate and product can be found in all DHODs (10–13,23,24). The specific roles of these residues in catalysis were unknown. The residues could be involved in binding both DHO and OA. They could also play a role in the chemical conversion of DHO to OA by stabilizing transition states and/or reaction intermediates or properly positioning DHO for the reaction. To try to better understand the roles these conserved residues play in DHO oxidation, site-directed mutagenesis was used. Removing hydrogen bonds from the active site can effect the reaction in several ways. Decreases in the reduction rate constant could be caused by altered substrate positioning, leading to slightly different relative orientations of the species involved in hydride transfer, or changes in the distance between the hydride donor (C6 of DHO) and hydride acceptor (N5 of FMN). Conversely, effects on the reduction rate constant could be due to the inability of the mutant enzyme to stabilize charge build-up of an intermediate or transition state during the reaction.

None of the mutations appeared to significantly disturb the environment of the flavin. Most of the mutant enzymes studied had reduction potentials nearly identical to that determined for wild-type (Table 1), the major exception being the Asn111Asp enzyme. The potential of this enzyme was ~100 mV lower than that of wild-type, consistent with the introduction of a negative charge at the active site. There is ample precedent for large effects on flavin potentials caused by altering the charge by mutation. For instance, the reduction potential of choline oxidase, another flavoprotein, was lowered by ~30 mV when a positively charged residue was mutated to neutrality, and by ~160 mV when the residue was mutated to a negatively charged residue (25).

The binding of OA suggests that the pyrimidine-binding site is largely intact in most of the mutant enzymes. Although the affinity for OA decreases (Table 2), the characteristic flavin spectral change (a red-shift from 456 nm to 475 nm) was usually observed. In the two most drastic mutations – Asn111Asp, where the charge of the active site was changed, and Asn172Ala/Asn246Ala, where three hydrogen-bonds were removed – the spectral changes

[2]The temperature was not properly controlled in the reactions of wild type and the Asn177Ala mutant enzyme, resulting in a temperature equilibration artifact (~1 s). The highly reproducible artifact was also observed in traces of buffer mixed with buffer and therefore was simply subtracted from all reaction traces. Because of this, the actual temperature of the experiment is unknown. However, the KIE observed with wild-type DHOD was very close to the previously published value for 4 °C, showing that there was a negligible temperature effect.

were less like wild-type, suggesting more significant perturbations to the active site and ligand binding, hardly a surprise.

Studying the reductive half-reaction of each mutant enzyme in anaerobic experiments gives information on the rate constant of flavin reduction (k_{red}) and the apparent K_d for DHO. The same KIE on flavin reduction was observed in all enzymes studied, indicating that the chemical step is not masked by another step, such as a slow isomerization, in these mutant enzymes, i.e., k_{red} truly indicates the rate constant for the chemical step. Furthermore, primary hydrogen isotope effects decrease as the forces in the transition state become less symmetric (26). None of the isotope effects on the reactions of the mutant enzymes decreased compared to wild-type. If mutations led to poor transition state geometry and therefore lower reduction rate constants, it is hard to imagine that symmetrical forces – needed to preserve the sizable isotope effects – would be maintained. Therefore, the KIE results argue that the decreases in reduction rate constants caused by the mutations were not due to suboptimal geometry.

Oxidized enzymes can bind both the substrate (DHO) and the product (OA) of the reductive half-reaction. The major difference in these two pyrimidines is their planarity – OA is planar, while DHO is not. When comparing the alanine single-mutations to wild-type, the range of effects observed on DHO binding was greater than that observed for OA binding (Figure 7). When Thr247 was mutated, the K_d values for DHO and OA were increased by nearly the same factor, indicating that Thr247 can bind both ligands equally well. Not only were the effects nearly equal, they were also some of the smallest effects observed in any of the mutant enzymes. Removal of other residues resulted in larger decreases in OA affinity than in DHO affinity. When Asn177 was mutated, no effect was observed on DHO affinity, while the K_d for OA increased ~8-fold. The Asn172Ala mutant enzyme was similar, with the K_d of DHO increased ~14-fold, while the K_d of OA increased ~65-fold. These residues seem more important for binding the planar ligand. In both the Asn246Ala and Asn111Ala mutant enzymes, bigger effects were observed on binding the non-planar DHO.

The observed effects on the reduction rate constant varied widely. There is no correlation between the observed K_d of DHO and the reduction rate constants (Table 3), i.e., the enzymes with the weakest K_d are not necessarily the slowest, suggesting that the range of effects is not simply the result of varying degrees of disruption of the active site structure. For example, the Asn177Ala mutant enzyme had the same apparent K_d as wild-type. However, the reduction rate constant of this mutant enzyme was reduced by nearly ~800-fold. Conversely, when Thr247 was mutated to alanine, the reduction rate constant was reduced by only ~8-fold, while the K_d of DHO increased by ~10-fold, so the Thr247Ala mutant enzyme binds DHO ~8-fold worse than the Asn177Ala mutant enzyme, but reacts ~80-fold faster. Binding – a thermodynamic property – and hydride transfer – the chemical step – are not linked, which is probably true of many enzymes.

Oxidation of DHO breaks two carbon-hydrogen bonds. An active site base (Ser175 in *E. coli* DHOD) deprotonates C5 of DHO and a hydride is transferred from C6 of DHO to N5 of the isoalloxazine ring of the flavin. Using DHO deuterated at the 5-, 6-, and both the 5- and 6-positions in anaerobic stopped-flow experiments, the *E. coli* DHOD was shown to use a stepwise mechanism in this reaction (5). Since DHO oxidation is stepwise in this enzyme, one of two intermediates must form during the reaction (Figure 8). If deprotonation occurs first, an enolate intermediate with negative charge on the C4 oxygen would form. If hydride transfer occurs first, an iminium intermediate with positive charge at the N1 position would form. Three of the four strictly conserved asparagine residues in DHOD hydrogen-bond to either the C4 carbonyl (Asn172 and Asn246 in *E. coli* DHOD) or N1 (Asn111 in *E. coli* DHOD) of DHO (Figure 1) and therefore are positioned to stabilize this potential charge build-up.

Removal of the hydrogen-bond(s) responsible for stabilizing the charge build-up of the intermediate by mutation to alanine should greatly decrease the rate constant of flavin reduction. Mutation of Asn246 results in only a ~570-fold decrease in the reduction rate constant, while a larger increase (~2,000-fold) in the apparent K_d for DHO is observed, indicating that this residue is more important for binding than for chemistry. Asn246 presumably hydrogen-bonds to both the C4 carbonyl and N3 of DHO. Therefore, replacement with alanine results in the loss of two hydrogen-bonds. If an equal contribution is assumed, then each hydrogen-bond accounts for ~2.3 kcal mol^{-1} in binding energy. With two hydrogen-bonds missing from the active site, it is likely that DHO is not held as rigidly in the proper orientation for chemistry. This would cause the observed decrease in reduction rate constant.

In contrast, mutation of Asn172 results in a large decrease in the reduction rate constant (10,500-fold), with only a minor increase in the K_d for DHO (~14-fold). This means that the hydrogen-bond provided by Asn172 is worth ~1.6 kcal mol^{-1} in binding energy. The large effect on chemistry implies that this residue is important for stabilizing transition states and/or reaction intermediates that form during the reaction. The observed effect supports the formation of an enolate during DHO oxidation. Interestingly, even though both Asn246 and Asn172 hydrogen-bond to the C4 carbonyl of DHO, Asn172 seems to be much more important for chemistry.

Surprisingly, mutation of Asn111 also results in a large decrease in reduction rate constant. In the Asn111Ala mutant enzyme, a ~4600-fold decrease in k_{red} is observed (~2-fold less than the effect observed in the Asn172Ala mutant enzyme). The effect on DHO binding is more significant in the Asn111Ala mutant enzyme with a ~50-fold increase in the K_d. This means that the hydrogen-bond contributed by Asn111 is worth ~2.4 kcal mol^{-1} of binding energy, very similar to the contribution of the hydrogen-bonds of Asn246. If an iminium intermediate is forming during DHO oxidation, negative charge near the N1 position of DHO should stabilize the positive charge build-up. Even though DHO binds very weakly to the Asn111Asp mutant enzyme, a reduction rate constant can be estimated. The chemical step in the Asn111Asp mutant enzyme occurs at ~0.1 s^{-1}, about 10-fold faster than in the Asn111Ala enzyme, although this rate constant is still ~450-fold slower than wild-type.

With large effects on reduction rate constant being observed when either Asn172 or Asn111 is removed, it is unclear which reaction intermediate is actually forming during DHO oxidation. However, it is clear that some of these conserved asparagine residues are important for chemistry in the Class 2 DHOD from *E. coli*; they are presumably needed to stabilize charge build-up in the active site during the reaction. The mechanism of DHO oxidation has also been studied in the Class 1A DHOD from *L. lactis*. In this instance, the deuterium isotope effects on flavin reduction indicated a concerted mechanism in which both carbon-hydrogen bonds break simultaneously (9). Interestingly, when the analogous asparagine residues in the *L. lactis* DHOD are mutated to alanine, the effects on flavin reduction are very mild, ranging from 40 – 200-fold (B. Tirupati, unpublished data). Thus, the mechanisms of DHO oxidation appear to be different in Class 1A and Class 2 DHODs and so do the effects of losing analogous active site asparagines. This is very likely due to differences in charge build-up in the active sites. In the Class 1A DHOD, presumably little charge build-up occurs because both bonds break simultaneously, and therefore small effects on the chemical step are observed when the active site asparagines are mutated.

While our data are consistent with at least some of the asparagines stabilizing charge build-up in the active site, it is still not clear which intermediate is forming in the stepwise oxidation of DHO by the Class 2 DHOD from *E. coli*. If an enolate intermediate is forming, loss of the hydrogen-bond to N1 should not slow reduction so severely because the charge build-up of an enolate intermediate is on the opposite end of the molecule. Conversely, if an iminium

intermediate is forming, then such a large effect from losing a hydrogen-bond at the C4 carbonyl is unexpected. Further work is needed to clarify which intermediate is formed.

The other two conserved active site residues are not positioned to stabilize intermediate formation. Thr247 hydrogen-bonds to the C2 carbonyl. When mutated to alanine, very minor effects are observed on both k_{red} and K_d. This is not surprising as this residue is proposed to bind and position DHO for catalysis, but not to stabilize any reaction intermediates. Asn177, the other strictly conserved asparagine residue, hydrogen-bonds to the carboxylate of DHO. The Asn177Ala mutation only affected the chemical step. This residue is located on the active site loop that is thought to be responsible for allowing access to the active site (11). Our results indicate that Asn177 is not responsible for binding DHO; that job belongs to the other conserved residues in the active site. It seems more likely that Asn177 is at least partially responsible for closing the active site lid once DHO is bound. The active site base (Ser175) that deprotonates C5 of DHO during the reaction is also on this active site loop. In order for the base to be positioned correctly, the loop must be closed over the active site (11). The decrease in the reduction rate constant upon mutation could be due to the inefficient closing of the active site loop in the absence of the hydrogen-bond between Asn177 and the carboxylate of DHO. It is also likely that Asn177 is needed to help properly position DHO for the reaction once it is initially bound. The reduction in k_{red} observed could be due to improper positioning of DHO in the active site.

The removal of each active site hydrogen-bond resulted in differential effects on the binding of DHO, OA, and the reduction of the enzyme-bound flavin. Some residues are more important for substrate binding, while others are extremely important for flavin reduction. Interestingly, the analogous mutations in another phylogenetic class of DHODs resulted in very different effects, suggesting that the conserved residues have different jobs in the different classes of DHODs. Intriguingly, our work shows important differences in FMN reduction between classes of DHODs, despite the active sites of the enzymes being nearly identical.

Supplementary Material

Refer to Web version on PubMed Central for supplementary material.

Acknowledgments

We thank Dr. Zainab Bello for the sample of purified Class 1B DHOD.

This work was supported by NIH Grant GM61087. RLF was supported by NIGMS training grant GM07767 and University of Michigan Rackham Graduate School Predoctoral Fellowship.

References

1. Björnberg O, Rowland P, Larsen S, Jensen KF. Active site of dihydroorotate dehydrogenase A from *Lactococcus lactis* investigated by chemical modification and mutagenesis. Biochemistry 1997;36:16197–16205. [PubMed: 9405053]
2. Jones ME. Pyrimidine nucleotide biosynthesis in animals: genes, enzymes, and regulation of UMP biosynthesis. Annu. Rev. Biochem 1980;49:253–279. [PubMed: 6105839]
3. Nagy M, Lacroute F, Thomas D. Divergent evolution of pyrimidine biosynthesis between anaerobic and aerobic yeasts. Proc. Natl. Acad. Sci. U. S. A 1992;89:8966–8970. [PubMed: 1409592]
4. Nielsen FS, Andersen PS, Jensen KF. The B form of dihydroorotate dehydrogenase from *Lactococcus lactis* consists of two different subunits, encoded by the pyrDb and pyrK genes, and contains FMN, FAD, and [FeS] redox centers. J. Biol. Chem 1996;271:29359–29365. [PubMed: 8910599]
5. Fagan RL, Nelson MN, Pagano PM, Palfey BA. Mechanism of flavin reduction in class 2 dihydroorotate dehydrogenases. Biochemistry 2006;45:14926–14932. [PubMed: 17154530]

6. Malmquist NA, Gujjar R, Rathod PK, Phillips MA. Analysis of Flavin Oxidation and Electron-Transfer Inhibition in *Plasmodium falciparum* Dihydroorotate Dehydrogenase. Biochemistry 2008;47:2466–2475. [PubMed: 18225919]
7. Palfey BA, Björnberg O, Jensen KF. Insight into the chemistry of flavin reduction and oxidation in *Escherichia coli* dihydroorotate dehydrogenase obtained by rapid reaction studies. Biochemistry 2001;40:4381–4390. [PubMed: 11284694]
8. Pascal RA Jr. Walsh CT. Mechanistic studies with deuterated dihydroorotates on the dihydroorotate oxidase from *Crithidia fasciculata*. Biochemistry 1984;23:2745–2752. [PubMed: 6087880]
9. Fagan RL, Jensen KF, Björnberg O, Palfey BA. Mechanism of flavin reduction in the class 1A dihydroorotate dehydrogenase from *Lactococcus lactis*. Biochemistry 2007;46:4028–4036. [PubMed: 17341096]
10. Liu S, Neidhardt EA, Grossman TH, Ocain T, Clardy J. Structures of human dihydroorotate dehydrogenase in complex with antiproliferative agents. Structure 2000;8:25–33. [PubMed: 10673429]
11. Nørager S, Jensen KF, Björnberg O, Larsen S. *E. coli* dihydroorotate dehydrogenase reveals structural and functional distinctions between different classes of dihydroorotate dehydrogenases. Structure 2002;10:1211–1223. [PubMed: 12220493]
12. Rowland P, Björnberg O, Nielsen FS, Jensen KF, Larsen S. The crystal structure of *Lactococcus lactis* dihydroorotate dehydrogenase A complexed with the enzyme reaction product throws light on its enzymatic function. Protein Sci 1998;7:1269–1279. [PubMed: 9655329]
13. Rowland P, Nørager S, Jensen KF, Larsen S. Structure of dihydroorotate dehydrogenase B: electron transfer between two flavin groups bridged by an iron-sulphur cluster. Structure 2000;8:1227–1238. [PubMed: 11188687]
14. Björnberg O, Gruner AC, Roepstorff P, Jensen KF. The activity of *Escherichia coli* dihydroorotate dehydrogenase is dependent on a conserved loop identified by sequence homology, mutagenesis, and limited proteolysis. Biochemistry 1999;38:2899–2908. [PubMed: 10074342]
15. Palfey, BA. Time Resolved Spectral Analysis. In: Johnson, KA., editor. Kinetic Analysis of Macromolecules. Oxford University Press; New York: 2003. p. 203-227.
16. Williams CH Jr. Arscott LD, Matthews RG, Thorpe C, Wilkinson KD. Methodology employed for anaerobic spectrophotometric titrations and for computer-assisted data analysis. Methods Enzymol 1979;62:185–198. [PubMed: 374972]
17. Massey, V. A simple method for the determination of redox potentials. In: Curti, B.; Ronchi, S.; Zanetti, G., editors. Flavins and Flavoproteins. Walter de Gruyter; Berlin, Germany: 1990. p. 59-66.
18. Nørager S, Arent S, Björnberg O, Ottosen M, Lo Leggio L, Jensen KF, Larsen S. *Lactococcus lactis* dihydroorotate dehydrogenase A mutants reveal important facets of the enzymatic function. J. Biol. Chem 2003;278:28812–28822. [PubMed: 12732650]
19. Marcinkeviciene J, Jiang W, Locke G, Kopcho LM, Rogers MJ, Copeland RA. A second dihydroorotate dehydrogenase (Type A) of the human pathogen *Enterococcus faecalis*: expression, purification, and steady-state kinetic mechanism. Arch. Biochem. Biophys 2000;377:178–186. [PubMed: 10775458]
20. Wolfe AE, Thymark M, Gattis SG, Fagan RL, Hu YC, Johansson E, Arent S, Larsen S, Palfey BA. Interaction of benzoate pyrimidine analogues with class 1A dihydroorotate dehydrogenase from *Lactococcus lactis*. Biochemistry 2007;46:5741–5753. [PubMed: 17444658]
21. Zameitat E, Pierik AJ, Zocher K, Löffler M. Dihydroorotate dehydrogenase from *Saccharomyces cerevisiae*: spectroscopic investigations with the recombinant enzyme throw light on catalytic properties and metabolism of fumarate analogues. FEMS Yeast Res 2007;7:897–904. [PubMed: 17617217]
22. Parsonage D, Luba J, Mallett TC, Claiborne A. The soluble alpha-glycerophosphate oxidase from *Enterococcus casseliflavus*. Sequence homology with the membrane-associated dehydrogenase and kinetic analysis of the recombinant enzyme. J. Biol. Chem 1998;273:23812–23822. [PubMed: 9726992]
23. Arakaki TL, Buckner FS, Gillespie JR, Malmquist NA, Phillips MA, Kalyuzhniy O, Luft JR, Detitta GT, Verlinde CL, Van Voorhis WC, Hol WG, Merritt EA. Characterization of *Trypanosoma*

brucei dihydroorotate dehydrogenase as a possible drug target; structural, kinetic and RNAi studies. Mol. Microbiol 2008;68:37–50. [PubMed: 18312275]

24. Inaoka DK, Sakamoto K, Shimizu H, Shiba T, Kurisu G, Nara T, Aoki T, Kita K, Harada S. Structures of *Trypanosoma cruzi* dihydroorotate dehydrogenase complexed with substrates and products: atomic resolution insights into mechanisms of dihydroorotate oxidation and fumarate reduction. Biochemistry 2008;47:10881–10891. [PubMed: 18808149]
25. Ghanem G, Gadda G. Effects of reversing the protein positive charge in the proximity of the flavin N(1) locus of choline oxidase. Biochemistry 2006;45:3437–3447. [PubMed: 16519539]
26. Westheimer FH. The Magnitude of the Primary Kinetic Isotope Effect for Compounds of Hydrogen and Deuterium. Chem. Rev 1961;61:265–273.

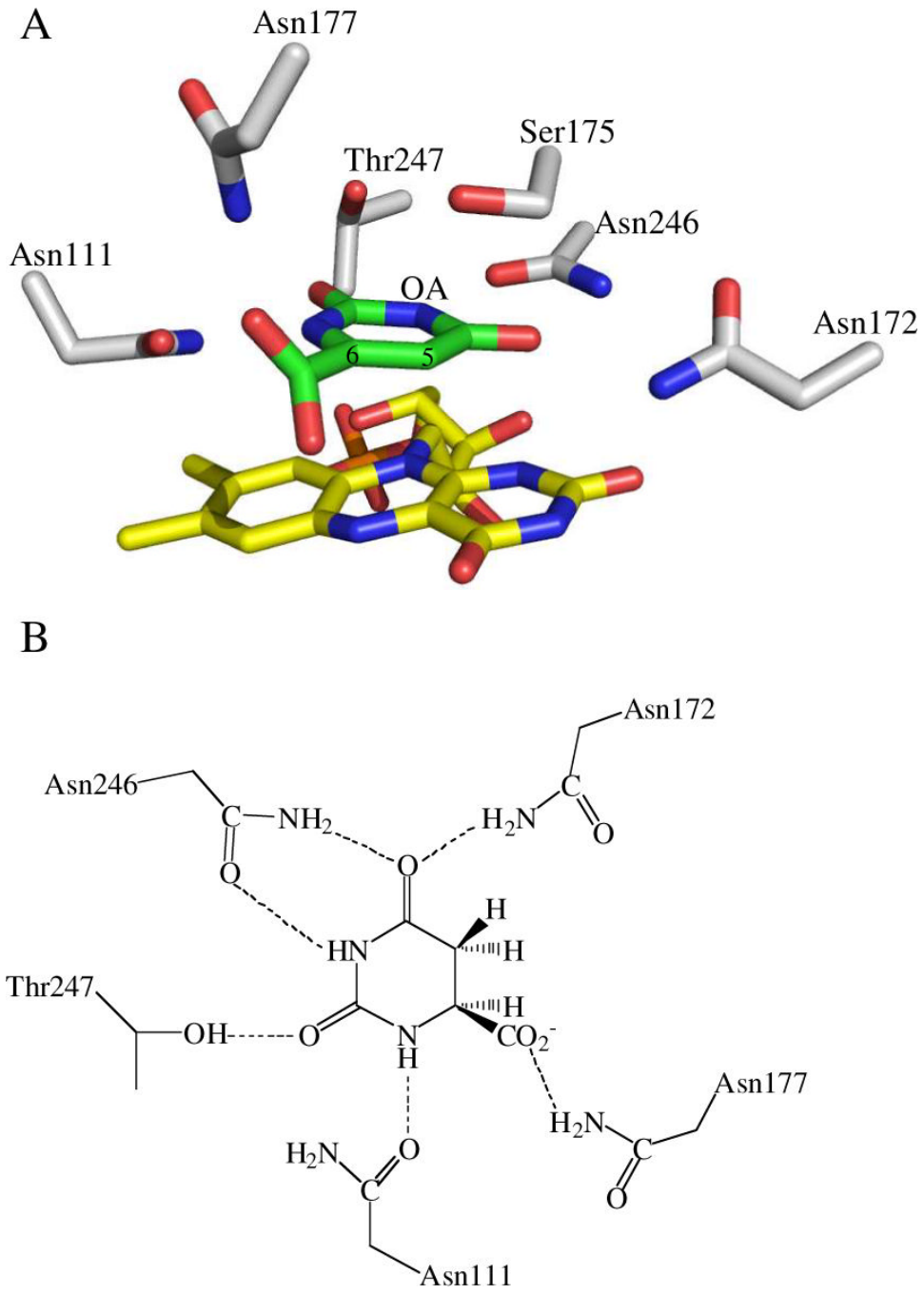

Figure 1.

Pyrimidine binding site of the Class 2 DHOD from *E. coli*. (A) The conserved hydrogen-bonding residues of the pyrimidine binding site are shown along with the active site base (Ser175). OA (green) stacks above the flavin with C6 in near van der Waals contact with N5 of FMN and C5 under the active site base. The flavin is shown in yellow. Coordinates taken from pdb file 1f76. (B) Schematic of the proposed hydrogen-bonds to DHO.

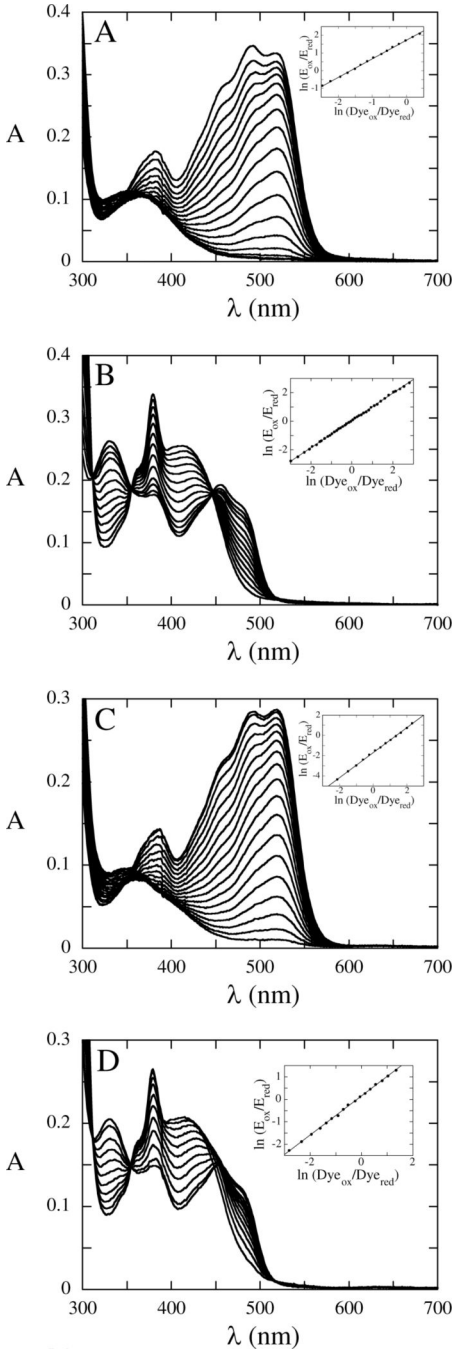

Figure 2.

Determination of reduction potentials. Reduction potentials were determined using the xanthine/xanthine oxidase method of Massey (17) in 0.1 M NaP_i, pH 7 at 25 °C. The reduction potential of wild-type *E. coli* DHOD was determined using phenosafranin (A) and 1-anthraquinone sulfonate (B). The reduction potential of the Asn246Ala mutant enzyme was also determined using phenosafranin (C) and 1-anthraquinone sulfonate (D). The insets in each panel show the Nernst plot for determining the potentials.

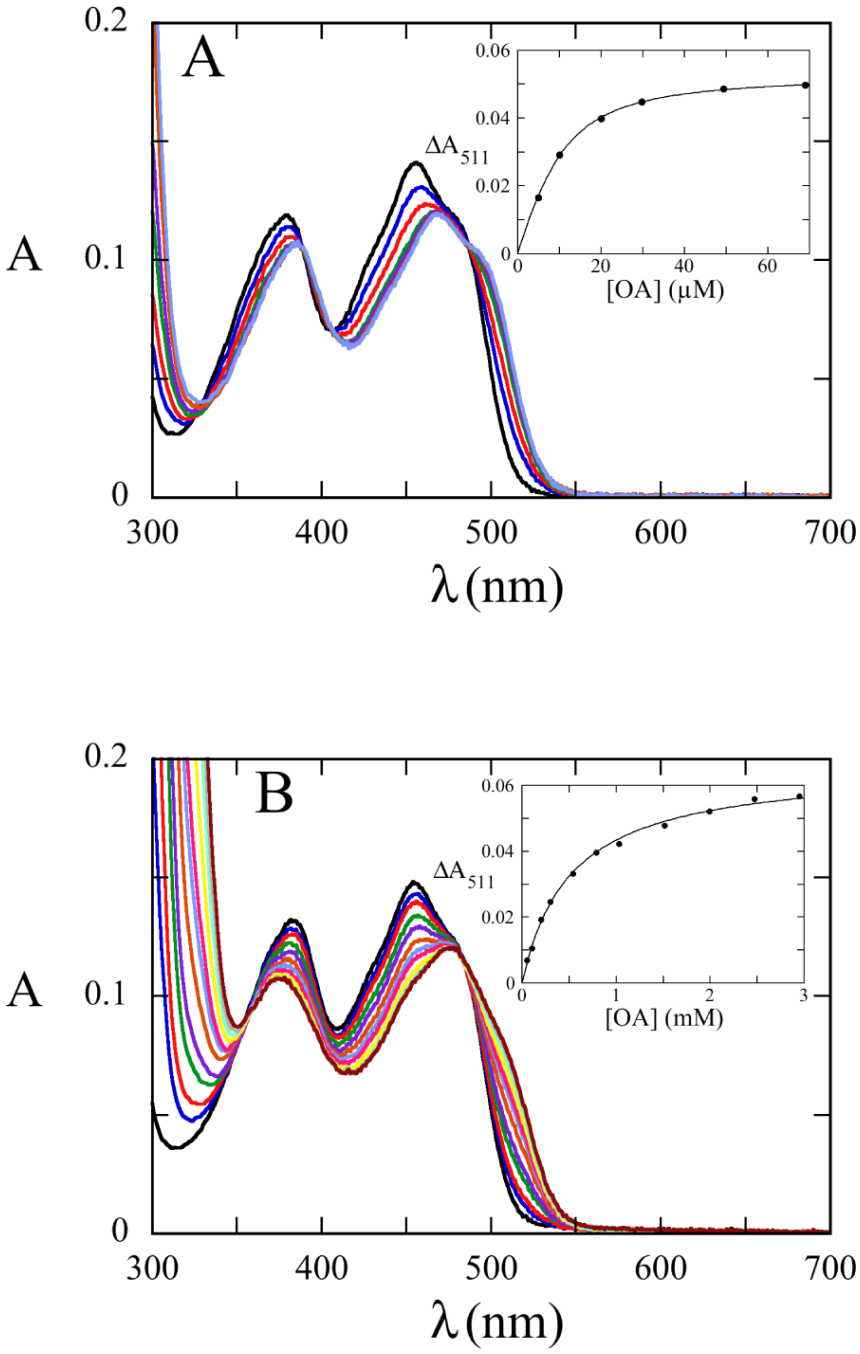

Figure 3.

OA binding titration, pH 8.5, 25 °C. The Thr247Ser mutant enzyme (A) and the Asn246Ala mutant enzyme (B) were titrated aerobically with OA. The inset shows the maximum change in absorbance due to OA binding as a function of OA concentration. Fitting to Eq 1 gives a K_d of 3.8 ± 0.5 μM for Thr247Ser (A). Fitting to a square hyperbola gives a K_d value of 520 ± 30 μM for Asn246Ala (B).

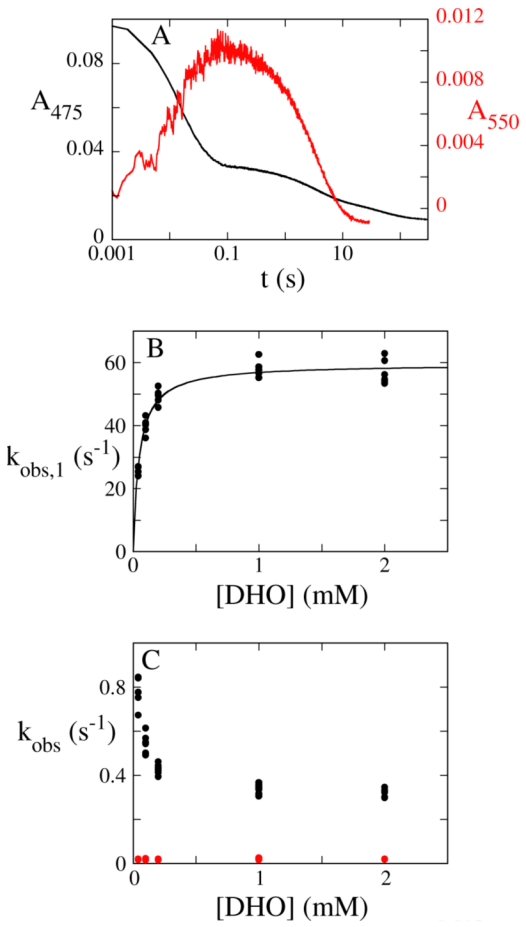

Figure 4.

Reductive half-reaction of Thr247Ser mutant DHOD. (A) Reaction traces observed when ~15 μM enzyme (before mixing) equilibrated in 0.1 M Tris, pH 8.5 was mixed with 4 mM DHO (before mixing) at 4 °C. At 475 nm (black), the reaction occurs in three phases. The first (large) phase represents the chemical step. The second phase represents product release. At 550 nm (red), flavin reduction is seen as an increase in absorbance and product dissociation is seen as a decrease in absorbance. The instrument dead-time (1 ms) has not been added to the times recorded in the traces. (B) The observed rate constant of the first phase (flavin reduction) saturates with increasing DHO concentration, giving a reduction rate constant (kred) of 58.8 ± 1.1 s^{-1} and a $K_{d,DHO}$ of 45 ± 5 μM. (C) Concentration dependence of the observed rate constant for the second and third phases. The observed rate constant of the second phase (black), OA release, decreases with increasing DHO concentration, giving a limiting value of 0.37 s^{-1}. The observed rate constant of the final phase (red) is ~0.02 s^{-1} and is independent of DHO concentration.

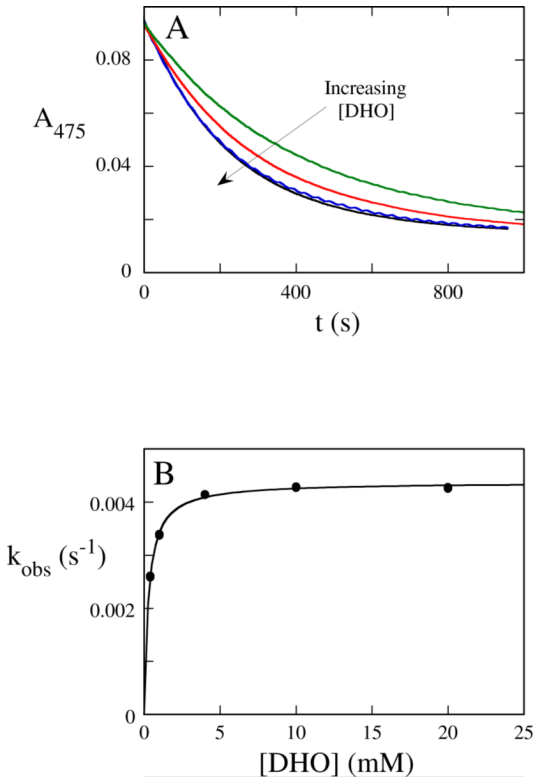

Figure 5.

Reductive half-reaction of the Asn172Ala mutant DHOD. (A) Reaction traces at 475 nm observed when ~14 μM enzyme (before mixing) was mixed with DHO ranging from 0.8 to 40 mM (before mixing) at pH 8.5, 4 °C. The instrument dead-time (1 ms) has not been added to the times recorded in the traces. (B) The observed rate constant varies hyperbolically with DHO concentration giving a k_{red} of 0.00437 ± 0.0002 s^{-1} and a $K_{d,DHO}$ of 278 ± 9 μM.

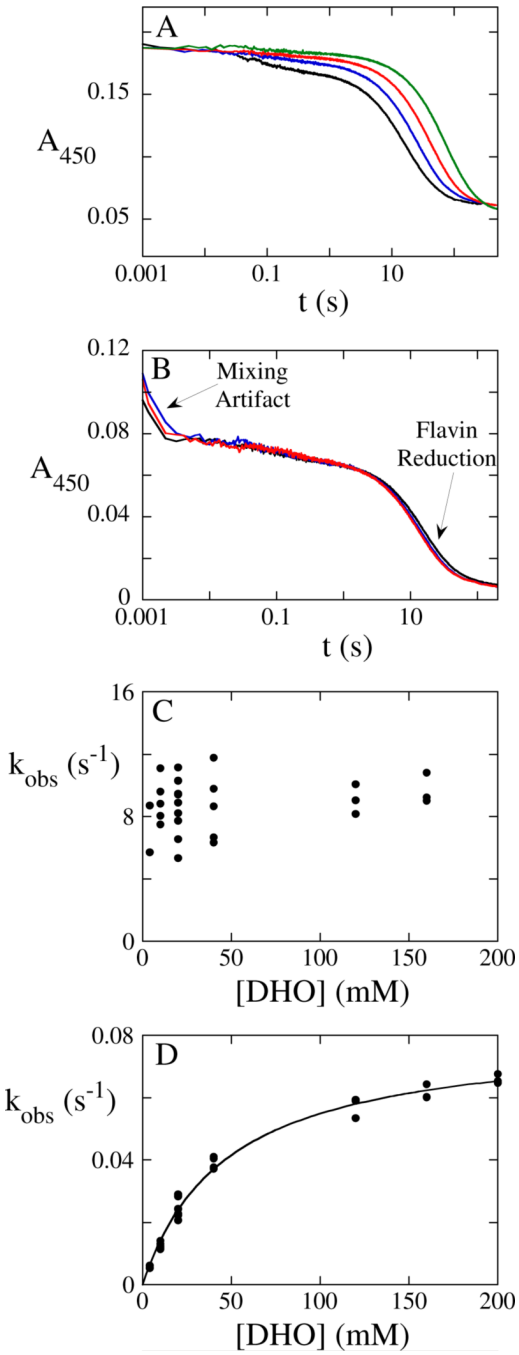

Figure 6.

Reductive half-reaction of the Asn246Ala mutant DHOD. (A) Reaction traces observed when ~29 μM enzyme (before mixing) was mixed with 20 – 48 mM DHO (before mixing) at pH 8.5, 4 °C. The instrument dead-time (1 ms) has not been added to the times recorded in the traces. (B) Reaction traces observed when ~12 μM enzyme (before mixing) was mixed with 240–400 mM DHO (before mixing) at pH 8.5, 4 °C. The mixing artifact is followed by two phases. The large second phase represents flavin reduction. (C) The observed rate constant of the first phase after the mixing artifact is independent of DHO concentration, with a k_{obs} scattered around ~9 s^{-1}. (D) The observed rate constant of the flavin reduction phase saturates with increasing DHO concentration giving a k_{red} of 0.081 ± 0.002 s^{-1} and an apparent K_d of DHO of 47 ± 3 mM.

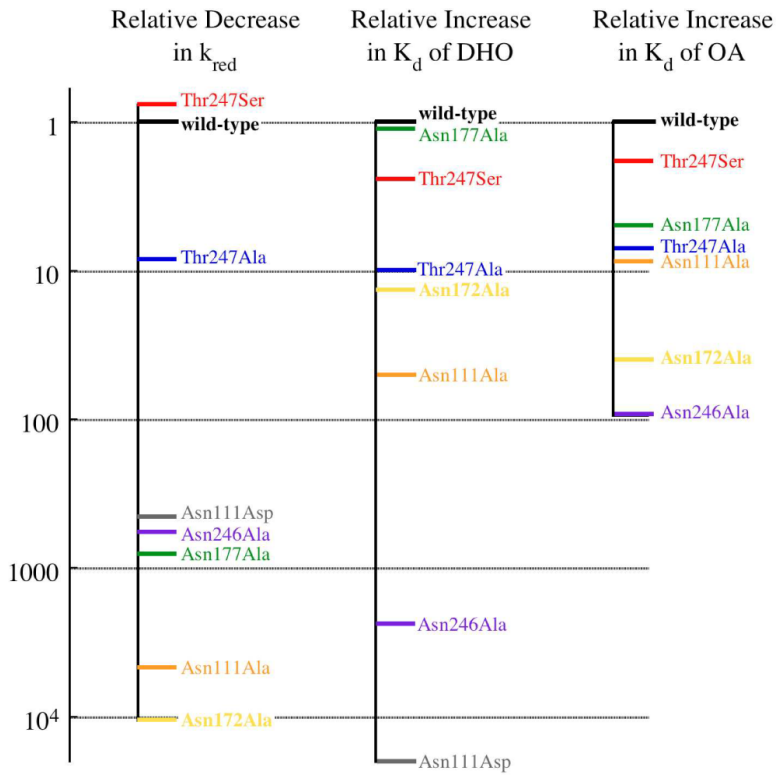

Figure 7.
Relative effects of all mutations. The effects of each mutation on the K_d of OA, the K_d of DHO, and the reduction rate constant with respect to wild-type is shown.

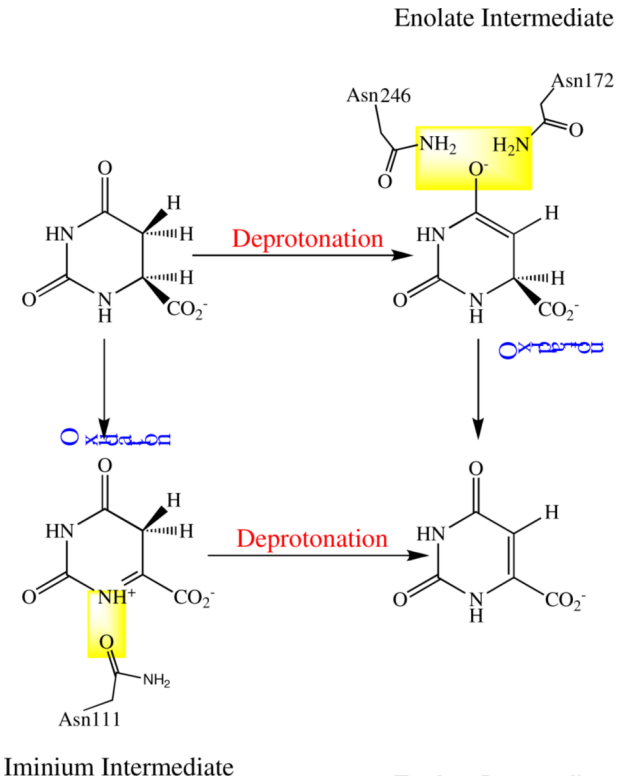

Figure 8.
Possible mechanisms of DHO oxidation. Class 2 DHODs oxidize DHO using a stepwise mechanism. One of two possible reaction intermediates occurs. Charge-stabilizing interactions of conserved active site residues are highlighted in yellow. Residues are positioned to stabilize either possible reaction intermediate.

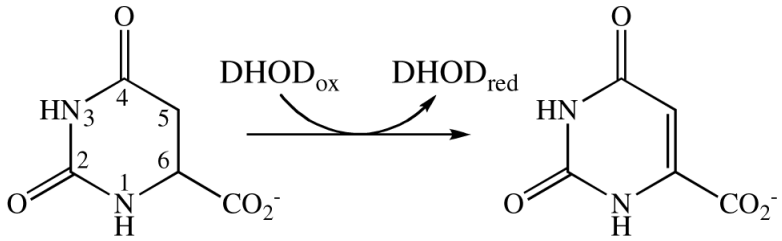

Scheme 1.

Scheme 2.

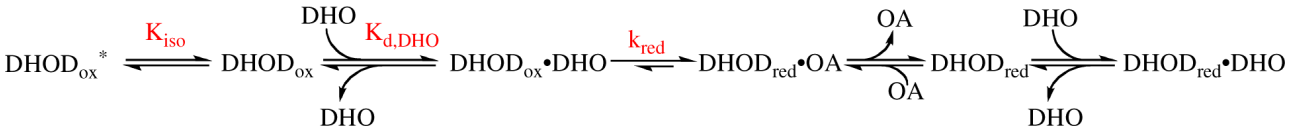

Scheme 3.

Table 1

Reduction Potentials of Wild-Type and Mutant *E. coli* DHODs

Enzyme	Reduction Potential
Wild-Type	−229 mV[a]
Thr247Ser	−229 mV[a]
Thr247Ala	−228 mV[a]
Asn177Ala	−258 mV[b]
Asn172Ala	−255 mV[b]
Asn246Ala	−233 mV[a]
Asn172Ala/Asn246Ala	−233 mV[a]
Asn11Ala	−238 mV[a]
Asn111Asp	−340 mV[c]

[a] Reduction potentials determined using both phenosafranin (E_m = −252 mV) and 1-anthraquinone sulfonate (E_m = −225 mV) and averaged.

[b] Reduction potential determined using only phenosafranin.

[c] Reduction potential determined using benzyl viologen (E_m = −350 mV).

Table 2

OA Binding to Wild-Type and Mutant Oxidized DHODs at pH 8.5, 25 °C

Enzyme	K_d (μM)	K_d(mutant)/K_d(Wild-Type)
Wild-Type	3.4 ± 0.8	-
Thr247Ser	3.8 ± 0.5	1.1
Thr247Ala	39.3 ± 1.6	12
Asn177Ala	27.5 ± 1.5	8
Asn172Ala	220 ± 9	65
Asn246Ala	518 ± 29	152
Asn172Ala/Asn246Ala	~ 50,000	~ 14700
Asn111Ala	47.2 ± 0.2	14
Asn111Asp	≫ 75,000	≫ 22000

Table 3

Reduction Rate Constants and Apparent $K_{d,DHO}$ for Active Site Mutant DHODs at pH 8.5, 4 °C

Enzyme	$K_{d,DHO}$ (μM)	k_{red} (S^{-1})
Wild-Type[a]	20	46
Thr247Ser	45 ± 5	58.8 ± 1.1
Thr247Ala	198 ± 16	5.52 ± 0.09
Asn177Ala	22 ± 2[b]	0.0586 ± 0.0004
Asn172Ala	278 ± 9	0.00437 ± 0.00002
Asn246Ala	47,000 ± 3,000	0.081 ± 0.002
Asn172Ala/Asn246Ala	~300 mM[c]	~0.002[b]
Asn111Ala	1,040 ± 60	0.0100 ± 0.0001
Asn111Asp	~ 400 mM	~0.1

[a] Data from reference (7).

[b] DHO concentrations low enough to decrease k_{obs} below half-maximal were not used, so the half-saturating value obtained from fits should only be considered to be a rough estimate.

[c] Determined at 25 °C.